CO5-1 Track observation in muscovite irradiated by ^{241}Am sources and its thermal stability

N. Hasebe, T. Nakashima[1], K. Miura[1], U. Uyangaa[1], G.Shuukhaaz[1], K. Oohashi[2], S.Akutsu[2], Y. Iinuma[3], and K. Takamiya[3]

Institute of Nature and Environmental Technology, Kanazawa University
[1]Graduate School of Natural Science and Technology, Kanazawa University
[2]Graduate School of Science and Technology for Innovation, Yamaguchi University
[3] Institute for Integrated Radiation and Nuclear Science, Kyoto University

INTRODUCTION: ^{238}U, ^{235}U, and ^{232}Th decay through emission of alpha particles to stable lead. Alpha Recoil Track (ART) is the damage created when daughter nuclides move back in reaction to alpha decay (Fleisher, 2003). Under the known decay constants of uranium and thorium, the age since the start of ART accumulation can be calculated by measuring the number of ARTs and uranium and thorium concentrations.
The purpose of this research is to establish a method to artificially form ARTs on mineral surfaces using muscovite ART detectors to help the understanding of ART behavior in various minerals. An experiment on the annealing behavior of ARTs in muscovite was also performed.

EXPERIMENTS: A 300 Bq americium source was tested to form artificial ART at Research Institute for Complex Nuclear Science, Kyoto University. Irradiation was performed under a vacuum at various time intervals (1 hour, 3 hours, 6 hours, 12 hours, 2 days, 4 days and 1 week). The ARTs were enlarged by etching with 47 % HF for two hours and observed with a phase contrast optical microscope.
Several samples of muscovite that have been irradiated for 3 hours were prepared and annealed at different temperatures (100℃, 150℃, 200℃) and times (30 min, 1 hour, 3 hours, 5 hours, 10 hours, 20 hours, 100 hours and 352 hours) to see the stability of ARTs under the geological condition.

RESULTS: The areal density of ARTs increased linearly against the irradiation time (Figure 1). One could identify each ART one by one in samples irradiated from 1 hour to 12 hours, but the number of ARTs formed on the muscovite surface was too many to identify for samples irradiated from 2 days to 1 week. Size of artificially formed ARTs (single alpha decay) was investigated and they were larger than natural ARTs (multiple alpha decay). In general, the artificial ART is formed by a single alpha decay from ^{241}Am to ^{237}Np. In contrast, muscovite without annealing should record the ARTs by multiple decay from the parent nuclide ^{238}U, ^{235}U, and ^{232}Th to the stable ^{206}Pb, ^{207}Pb, and ^{208}Pb, respectively, so that one can expect larger natural tracks than the artificial tracks formed by irradiation.
Based on the annealing experiment, It was concluded that natural ARTs were annealed at ambient temperature for a long period of time because the size of ART tends to decrease with annealing time during the isothermal annealing experiment (Figure 2). The establishment of the artificial ART formation method will make it possible to observe the shape and characteristics of ARTs in various minerals other than mica and will contribute to further development of geochronological use of ART, especially including zircon.

REFERENCES:

[1] Fleischer R., Geochim. cosmochim. acta, **67**, (2003) 4769-4774.

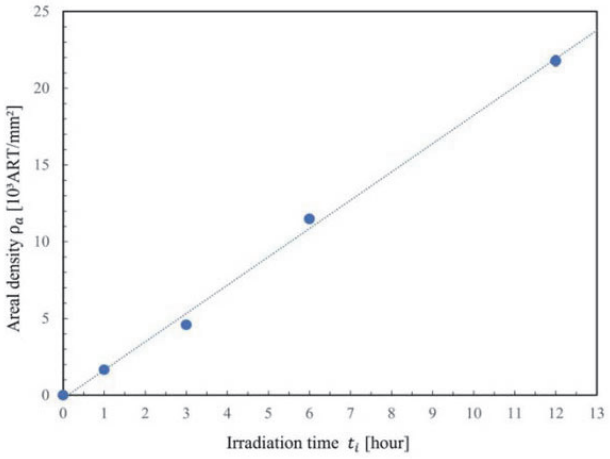

Fig. 1. Areal density of ARTs is plotted against irradiation time.

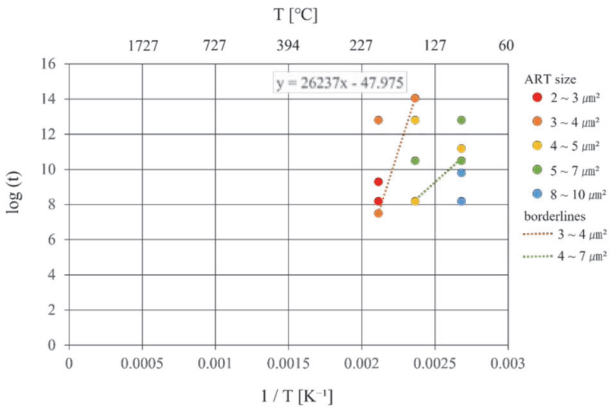

Fig. 2. The Arrhenius plot based on the annealing temperatures and times (sec).

CO5-2 Mechanisms of high-pressure transitions in $(Mg,Fe)_2SiO_4$ under differential stress

N. Tomioka[1], T. Okuchi[2], M. Miyahara[3]

[1]*Kochi Institute for Core Sample Research, Japan Agency for Marine-Earth Science and Technology*
[2]*Institute for Integrated Radiation and Nuclear Science, Kyoto University*
[3]*Graduate School of Advanced Science and Engineering, Hiroshima University*

INTRODUCTION:

Phase equilibria studies have demonstrated that olivine [$(Mg, Fe)_2SiO_4$: α-phase] transforms into a spinelloid structure (wadsleyite:β-phase) and then into a spinel structure (ringwoodite: γ-phase) with increasing pressure. Natural examples of wadsleyite and ringwoodite were first discovered in heavily shocked meteorites. Based on the characterizations of planer defects in these natural phases, shear-promoted "diffusionless" mechanisms were proposed in transformations among the olivine polymorphs [1]. The transformation models also predicted the possible occurrence of an intermediate phase, which is exhibiting the smallest unit cell among all spinel/spinelloid structures. We recently discovered the phase as a mineral poirierite (ε-phase) in shocked meteorites [2, 3]. In the present study, we have carried out a transformation experiment on olivine to understand the conditions and mechanism of the poirierite formation.

EXPERIMENTS:

Natural olivine with an Fe/(Mg+Fe) ratio of 0.09 was used in the transformation experiments. The olivine single crystal was crushed into powder with heterogeneous grain size less than 100 μm. The powder was kept at 16 GPa and 900 °C for 2 hours by using a Kawai-type high-pressure apparatus. The recovered samples were measured using an X-ray diffractometer (RIGAKU SmartLab 9 kW) at the Institute for Integrated Radiation and Nuclear Science, Kyoto University. The X-ray beam is focused to a diameter of ~100 μm. The portions at the reaction boundaries were extracted and to be ultrathin sections of ~150 nm in thickness by using a focused ion beam apparatus (Hitachi SMI-4050), and then examined by a transmission electron microscope (TEM: JEOL JEM-ARM200F).

RESULTS AND DISCUSSION:

The olivine grains are partially transformed at their grain boundaries. Micro-area powder X-ray diffraction patterns show that the product phase is exclusively ringwoodite (Fig. 1). The ringwoodite occurs as euhedral and subhedral crystals with a grain size of 490 ± 270 μm under TEM (Fig. 2). Most of the ringwoodite grains exhibit pervasive stacking faults on {110} planes. These defects have also been reported in ringwoodite in shocked meteorites [e.g. 2,3]. The selected-area electron diffraction (SAED) patterns of many ringwoodite grains with a high density of planar defects show weak extra diffraction spots corresponding to poirierite. In addition, the SAED patterns of the ringwoodite-poirierite intergrowth show that both phases have a topotaxial relationship: $(001)_\varepsilon$//$\{001\}_\gamma$ and $(100)_\varepsilon$//$\{110\}_\gamma$. The relict olivine has a high dislocation density of 1.4 x 10^9 /cm^2, corresponding to a differential stress of ~0.6 GPa according to an olivine piezometer [4].

Microstructural and crystallographic features of the sample described above suggest that polycrystalline ringwoodite grains were formed by a nucleation and growth mechanism at grain boundaries of olivine, while poirierite lamellae were metastably formed within ringwoodite grains by a shear mechanism. The latter transformation would be favored by relatively low temperature conditions, where atomic diffusion is kinetically hindered, and by high differential stress, which causes shearing of the oxygen sublattices of the spinel/spinelloid structures. The transformation experiments at different pressure conditions are currently ongoing.

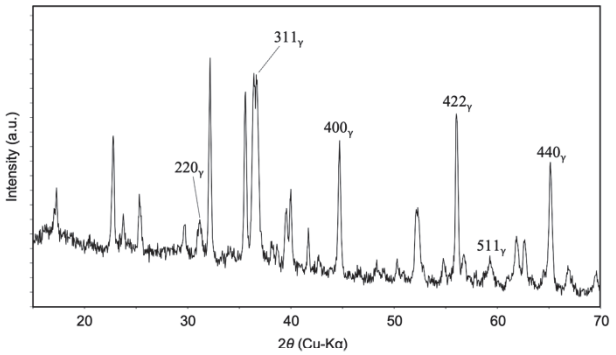

Fig. 1. Micro-area X-ray diffraction pattern taken from olivine kept at 16 GPa and 900 °C. Peaks with notations are from ringwoodite (γ), and all the other peaks are from olivine.

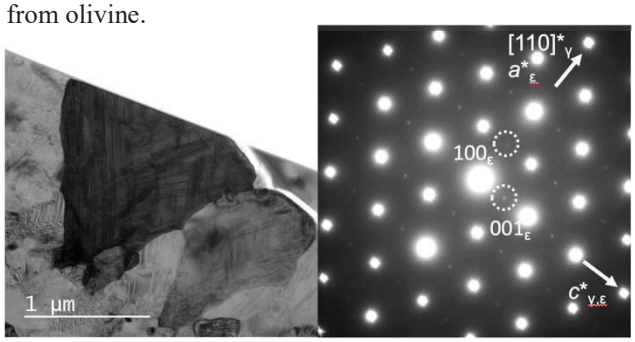

Fig. 2. Transmission electron micrograph (Left) and selected-area electron diffraction patten (Right) of a ringwoodite (γ) grain with intergrown poirierite (ε).

REFERENCES:

[1] M. Madon and J. P., Poirier, Phys. Earth Planet Inter., **33** (1983) 31–44.
[2] N. Tomioka and T. Okuchi, Sci. Rep., **7** (2017) 17351.
[3] N. Tomioka *et al.*, Commun. Earth Environ., **2**, (2021) 16.
[4] Kohlstedt *et al.* (1976). in Physics and Chemistry of Minerals and Rocks, R. G. J. Strens (ed.), (1976) 35–49.

CO5-3 Experimental evaluation of impact-induced structure transformation of planetary minerals

T. Okuchi, N. Tomioka[1], Y. Seto[2], Y. Umeda and T. Sekine[3]

Institute for Integrated Radiation and Nuclear Science, Kyoto University

[1]Kochi Institute for Core Sample Research, Japan Agency for Marine-Earth Science and Technology

[2]Graduate School of Science, Osaka Metropolitan University

[3]Center for High Pressure Science & Technology Advanced Research

INTRODUCTION: 4.6 billion years ago in a nebula surrounding the primordial sun, numerous small bodies were growing into planets and satellites through their mutual collisions. After the collisions of small bodies, some evidences had been recorded within themselves to indicate their impact histories, where materials were strongly and temporally compressed during the impact events. A typical example of such evidence is frozen dense structures occurring after such compression, which emerged through structural transformations of the mineral crystals that originally consisted the asteroids.

There are numbers of previous reports on such dense structures occurring in primitive meteorites [1]. We have been reporting some of these structures including newly discovered one, which had been very possibly recording hypervelocity impact events of the ancient asteroids [2,3]. In these meteorites, we observed that low-density olivine crystals [α-$(Mg,Fe)_2SiO_4$] were transformed into one or more of its three dense high-pressure polymorphs. These are of particular interest because they could have recorded the timescale and the pressure scale of the ancient impact processes in quantitative manner [2,3].

The purpose of the current research is to reveal the formation mechanisms of these dense mineral structures as unique evidences of evolution history of the early solar system, with particular attention to their nanoscale morphological structures and textures.

RESULTS: We experimentally evaluated the timescales of such planetary shock events and also their generated pressure scales. For that purpose, we observed the structure transformation process from α-Mg_2SiO_4 into one or more of its dense high-pressure polymorphs during experimentally-induced shock compression events, which results in an ultrafast structure transformation into ringwoodite [γ-Mg_2SiO_4] [4]. Ringwoodite is one of the most-commonly observed dense high-pressure polymorph minerals occurring in deformed primitive meteorites. For conducting this experiment, we focused a high-power laser pulse into α-Mg_2SiO_4 to apply strong shock compression, where its transformation process was time-resolved by ultrafast diffractometry using a x-ray free electron laser pulse of femtosecond time width generated at SACLA facility [5]. We observed a lattice-shear mechanism which was proceeded within several nanoseconds, much faster than any previous estimation of solid-state structure transformation mechanism of silicate minerals. The mechanism proceeded even during short-lived shocks equivalent to those induced by impacts of relatively-small (sub-kilometer-scaled) asteroids. The mechanism mostly worked during shock releases, such that the peak shock pressures deduced from the existence of shear-induced olivine polymorphs could be underesti-mated. Since shorter-duration compression events occur more frequently in asteroid impacts, the shorter events could have more frequently recorded the fast mechanism. When we carefully search for such records in meteorites and asteroids, we will be able to quantitatively recon-struct the evolution history of the early solar system through numerous impact events.

REFERENCES:

[1] M. Miyahara *et al.,* Prog. Earth Planet. Sci., **8** (2021) 59.
[2] N. Tomioka and T. Okuchi, Sci. Rep., **7** (2017) 17351.
[3] N. Tomioka *et al*., Commun. Earth. Environ., **2** (2021) 16.
[4] T. Okuchi *et al*., Nat. Commun., **12** (2021) 4305.
[5] T. Okuchi, SPring-8/SACLA Information, **26** (2021) 341-348.

CO5-4 Volcanic and Tectonic History of Philippine Sea Plate (South of Japan) Revealed by $^{40}Ar/^{39}Ar$ Dating Technique

O. Ishizuka, S. Sekimoto[1], R. Okumura[1], H. Yoshinaga[1], Y. Iinuma[1], T. Fujii[2]
Geological Survey of Japan, AIST
[1]Institute for Integrated Radiation and Nuclear Science, Kyoto University
[2]Graduate School of Engineering, Osaka University

INTRODUCTION:

Robust tectonic reconstruction of the evolving Philippine Sea Plate for the period immediately before and after subduction initiation at ~52 Ma to form the Izu-Bonin-Mariana arc is prerequisite to understand cause of subduction initiation. Understanding of nature and origin of overriding and subducting plates is especially important because plate density is a key parameter controlling subduction initiation based on numerical modelling. There is increasing evidence that multiple geological events related to changing stress fields took place in and around Philippine Sea plate about the time of subduction initiation at ~52 Ma [1]. To understand tectonics during the period of subduction initiation, it is important to understand the pattern and tempo of these geological events, particularly the duration and extent of seafloor spreading in the Mesozoic arc terrane (Daito Ridge Group), and its temporal relationship with spreading in the West Philippine Basin (WPB).

In this study we have investigated magmatism in the oldest part of the Philippine Sea Plate to reveal for the first time the age and origin of the northernmost part of the WPB and the Palau Basin. The outcome of these studies will assist in understanding the time sequence of magmatic and tectonic events which took place within a relatively short period around 52 Ma, i.e., immediately before and after subduction initiation along the Pacific margin.

EXPERIMENTS: Ages of the igneous rocks were determined using the $^{40}Ar/^{39}Ar$ dating facility at the Geological Survey of Japan/AIST. 10-15 mg of phenocryst-free groundmass, crushed and sieved to 250 – 500 μm in size, was analyzed using a stepwise heating procedure. The samples were treated in 6N HCl for 30 minutes at 95°C with stirring to remove any alteration products (clays and carbonates) present in interstitial spaces. After this treatment, samples were examined under a microscope. Sample irradiation was done either at the Kyoto University Reactor (KUR). The neutron irradiation was performed for 10 h at the hydro-irradiation port under 1 MW operation, where thermal and fast neutron fluxes are 1.6×10^{13} and 7.8×10^{12} n/ cm^2 s, respectively, or for 2 h under 5 MW operation, where thermal and fast neutron fluxes are 8.15×10^{13} and 3.93×10^{13} n/cm^2 s respectively. Argon isotopes were measured in a peak-jumping mode on an IsotopX NGX noble gas mass spectrometer fitted with a Hamamatsu Photonics R4146 secondary electron multiplier.

RESULTS: 6 samples have been dated by the laser-heating $^{40}Ar/^{39}Ar$ dating technique. Basalts from the basin floor of northernmost part of the WPB show age range between 47.5 and 49.3 Ma (Fig.1). Basalts from the Palau Basin gave age range between 45.2 and 48 Ma.

SUMMARY:

1) The new dating results from the oldest part of the WPB and the Palau Basin strongly imply that these ocean basins which are supposed to form the oldest part of the Philippine Sea Plate only formed mostly after c. 51 Ma.

2)This fact seems to provide further support for the model that the Izu-Bonin-Mariana arc was established on ocean crust formed associate with subduction initiation, but not on the older ocean crust existed prior to the subduction initiation [2]. This also confirm that the overriding plate at subduction initiation (i.e., Philippine Sea Plate) is mainly composed of Mesozoic remnant arc terrane represented by the Daito Ridge Group, and might have had not much ocean crust.

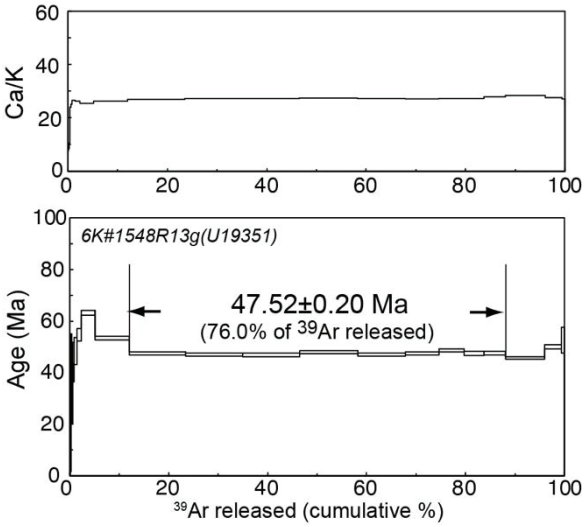

Fig. 1. Age spectrum for the basalt from the northernmost part of the WPB.

REFERENCES:

[1] O. Ishizuka *et al.*, Earth and Planet. Sci. Lett., **306** (2011) 229-240.
[2] O. Ishizuka *et al.*, Earth and Planet. Sci. Lett., **481** (2018) 80-90.

CO5-5 Temporal trends of extractable organochlorine in wild kite (*Milvus migrans*)

K. Ito[1], T. Fujimori[2], K. Oshita[1], S. Fukutani[3], H. Mizukawa[4], M. Takaoka[1], S. Takahashi[4]

[1]*Department of Environmental Engineering, Graduate School of Engineering, Kyoto University*

[2]*Faculty of Advanced Science and Technology, Ryukoku University*

[3] *Institute for Integrated Radiation and Nuclear Science, Kyoto University*

[4] *Graduate School of Agriculture, Ehime University*

INTRODUCTION: Among organochlorine compounds, persistent organic pollutants (POPs) are subject to international regulation, but the number of POPs and the diversity of alternatives and analogues with similar properties is increasing, so extractable organochlorine (EOCl) have attracted attention as a comprehensive risk assess-ment [1]. POPs are known to be concentrated in highly trophic animals through bioaccumulation in the food chain, and wild birds are considered one of the most sen-sitive organisms to pollutants.

The aim of this study is to temporally evaluate EOCl in archived wild kite liver samples. Extracts were separated by 1000 g/mol molecular weight and measured by neu-tron activation analysis (NAA) and compared to poly-chlorinated biphenyls (PCBs) concentrations in the same samples reported previous study [2] to quantitatively evaluate unidentified chlorine.

EXPERIMENTS: Kite liver samples were used from individuals which were collected at Matsuyama airport from 1977 to 2018. Samples were dissected after collec-tion and stored frozen in environmental specimen bank (*es*-BANK) in Ehime university.

The extraction method followed previous studies [1]. Samples were extracted in organic solvents using homogenizer and washed with aqueous solution. Gel permeation column chromatography was used to fractionate at a molecular weight of 1000 g/mol (lower fraction is EOCl-L), and the extract was places in polyethylene (PE) bags and dried under normal temperature and pressure. Samples were irradiated for 15 min with a thermal neutron flux of $2.0–2.4\times10^{13}$ cm^{-2} · S^{-1} at KURNS. ^{38}Cl ($t_{1/2}$ = 37.18 min, E_γ = 1642, 2168 keV) were measured by using a Ge semiconductor detector for 300 sec. Concentrations in the samples were calculated using the comparison method between those and standard samples minus the amount of chlorine from the PE bag.

RESULTS: Figure(A) shows the results of EOCl-L in kite liver samples. EOCl-L averaged 15.9 ± 18.9 μg/g lipid overall. The concentrations of EOCl-L were decreased from 1977 to 1990. This may reflect a decrease in PCBs due to environmental regulations. On the other hand, no large changes were observed for both EOCl-L and PCBs after 2001. The indicated that in addition to PCBs remaining in the environment, the compounds in EOCl-L have not changed much. And it is possible that the compounds of anthropogenic origin have been present for a long time.

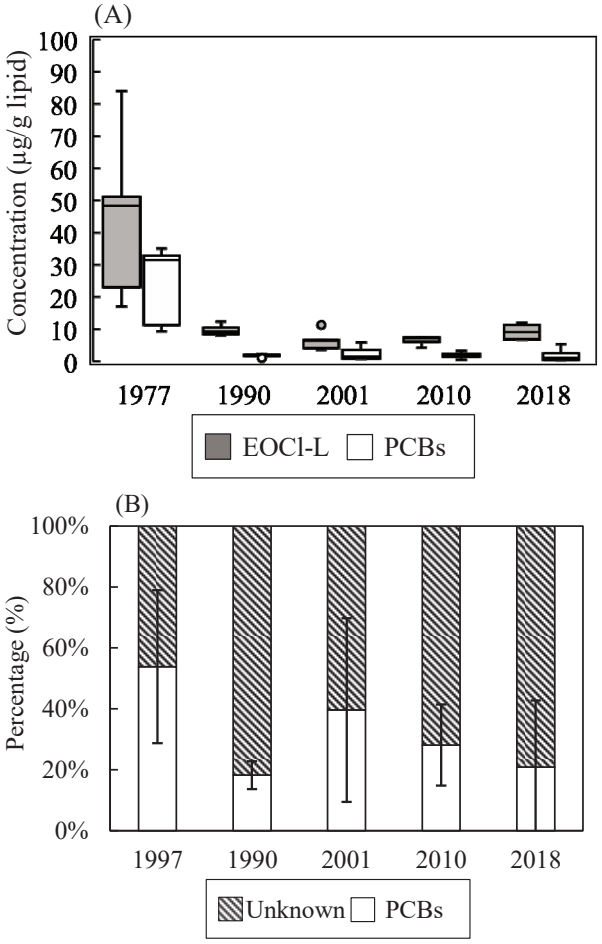

Figure(A) is the concentrations of EOCl-L and PCBs, and **Figure(B)** is the percentage of unknown Cl and PCBs in kite liver samples.

In the **Figure(B)**, the percentage of unidentified chlorine (i.e. EOCl-L - PCBs) in EOCl-L were about 50 %. The concentration of EOCl-L was also high in this year, suggesting that environmental contamination by chlorinated pesticides and other compounds had an impact for environment. In addition, the percentage of unidentified samples has been increasing since 2000, and in 2018, about 80 % of the EOCl-L were unidentified, so futher attention should be paid to this issue.

From this study, we were able to quantitatively evaluate the time change of EOCl-L and unidentified chlorine in kite liver samples. The results indicate that the threat from unidentified compounds is lower than in 1977, but the unidentified percentage has increased in recent years, suggesting the need for regular monitoring.

REFERENCES:

[1] K. Mukai *et al.*, Science of the Total Environment., **756** (2021) 143843.

[2] Watanabe *et al.,* (2021) 29th Symposium on Environmental Chemistry. Osaka, Japan.

CO5-6 Determination of Uranium in Local Fallout from A-bomb Using Fission-Track Analysis

K. Takamiya, N. Toe, M. Inagaki, Y. Oki and Y. Igarashi

Institute for Integrated Radiation and Nuclear Science, Kyoto University

INTRODUCTION: The distribution and properties of fallout materials those were released into the environment by atomic bombs and deposited on the ground surface is important to estimate exposure dose from residual radiation of the atomic bomb, as typified by the black rain. Measurements and determination of ^{137}Cs in fallout materials have been tried for collecting soil samples. However, since the origin of ^{137}Cs includes not only the atom-ic bomb fallout but also the fallout from atmospheric nuclear tests conducted around the world after 1950's, it is very difficult to identify its origin. Therefore, we considered the possibility of using insoluble particles containing uranium as an indicator of the atomic bomb-derived local fallout. Many insoluble particles containing radioactive cesium and uranium were found in the TEPCO Fukushima Daiichi Nuclear Power Plant accident [1], and similar insoluble particles could be produced by the atomic bombs. Therefore, we attempted to detect uranium-containing particles in soil using fission track method, which is used to detect trace amounts of uranium.

EXPERIMENTS: If particles in the soil contain high concentrations of uranium, these particles might have a higher specific gravity than general soil particles. Therefore, in order to efficiently detect particles containing uranium, we developed a method that combines heavy liquid separation and the fission track method [2, 3]. A sodium polytungstate (SPT) solution was used for heavy liquid separation. A part of soil sample collected in Hiroshima was mixed with SPT solution adjusted to 3.0 g/cm^3, and centrifuged at 3000 rpm for 10 minutes at room temperature to separate particles with a specific gravity more than 3.0 g/cm3. The separated particles were collected on a PTFE filter and attached to a track detector (BARYOTRAK-P, Fukuvi Chemical Industry Co., Ltd.) and wrapped by a paraffin film. Particles and the track detector were irradiated by about 3.10^{14} n/cm^2 of thermal neutrons using the pneumatic irradiation facility (TC-Pn) at Kyoto University Research Reactor. After the irradiation, the particles and filter were removed from the track detector together with the paraffin film, the surface was washed with pure water, and then etched with 8 M NaOH at 70 °C for 1 hour.

RESULTS: If a particle containing a high concentration of uranium exists, it is expected that tracks were observed radially around the particle. Fig. 1 shows an example of the results of an analysis of soil samples collected at the area where the black rain phenomenon was observed in Hiroshima Prefecture. At least two clusters of tracks can be detected in this figure. The enlarged image of the right cluster of Fig. 1 was shown in Fig. 2. The size of the particle forming the cluster in Fig. 2 is estimated to be several tens of μm. Many similar cluster of tracks were also detected in soil samples collected at the same point at different ground depths. On the other hand, such a cluster was not detected for fallout samples collected in Japan after 1960 by using similar fission track method. Therefore, the origin of this particle might not be an atmospheric nuclear test. In addition, very few clusters of tracks were detected for soil samples collected at locations about 20 km east from the hypocenter. Therefore, it is considered that the particles forming the clusters of numerous fission tracks in this experiment includes fallout materials derived from the atomic bomb.

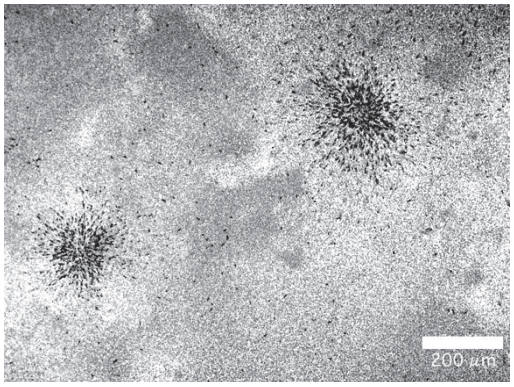

Fig. 1. Clusters of fission tracks observed on a track detector by neutron irradiation.

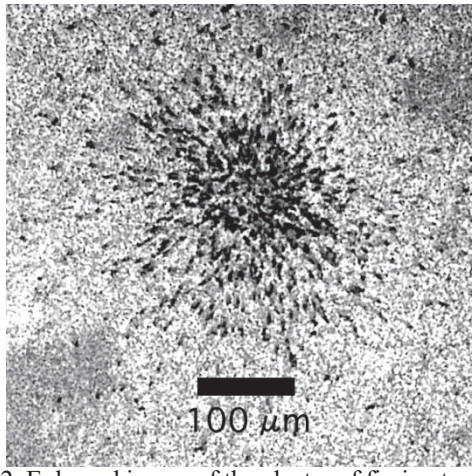

Fig. 2. Enlarged image of the cluster of fission tracks.

REFERENCES:

[1] Y. Abe *et al.,* Anal. Chem., **86** (2014) 8521-8525.
[2] K. Iguchi, J. Soc. Photogr. Sci. Tech. Jpn., **6** (2005) 59.
[3] F. Esaka *et al.*, Anal. Chem., **87** (2015) 3107-3113 .

CO5-7 Trace elements and Ar-Ar analyses of extraterrestrial materials

R. Okazaki[1], S. Sekimoto[2], N. Shirai[3], and J. Park[4]

[1]*Department of Earth and Planetary Sciences, Kyushu University*

[2]*Institute for Integrated Radiation and Nuclear Science, Kyoto University*

[3]*Department of Chemistry, Tokyo Metropolitan University*

[4]*Kingsborough Community College, the City University of New York*

INTRODUCTION: Meteorites and cosmic dust (micrometeorites) have diverse mineralogical, chemical, and isotopic compositions, which records their origins and evolution histories. Mineralogy and major element compositions can be obtained using commonly-used instruments, such as an electron micro-prove analyzer, whereas some of trace elements and Ar-Ar analyses require neutron irradiation. We have developed the analytical method to determine trace element compositions and Ar-Ar ages of individual submillimeter-sized extraterrestrial materials. This method has been applied to the Hayabusa2 samples in Projects #R3007, R3038, and R3127 using the Hydro irradiation in 2021.

EXPERIMENTS: Plagioclase and pyroxene mineral separates of 0.15-0.7 mg in weight were prepared from 7 eucrites (Agoult, HaH262, Yamato-792510, Y-792769, Y980318, Y980433, and Y983366) and a shergottite (Y002712). Bulk meteorite samples of 0.3-0.7 mg in weight (A12325 and Y002712 shergottites, DEW12007 lunar meteorite, NWA12542 nakhlite, and NWA8785 EH3 chondrite) were also prepared. The Allende CV chondrite (Provided by Smithonian museum [1]) of 0.07 mg and terrestrial minerals (orthoclase [2] and wollaston-ite) were used as the laboratory standards. Each of the samples was placed in a conical dimple (φ1, depth ~ 0.5 mm) of a sapphire disk (φ5.5, 1.5 mm thick), and covered with a sapphire disk (φ5.5, 0.3 mm thick). Each of the sapphire container was wrapped with pure aluminum foil. These Al-wrapped containers were stacked (Fig. 1) and sealed in the capsules for the Hydro irradiation. The irra-diation was operated at 1 MW for 47 h plus 5 MW for 6 h.

REUSLTS and DISCUSSION: The meteorite samples and the standard samples were irradiated in the Hydro irradiation term of Jan. 2023. One month later (on March 14-16), the irradiated samples were removed from the irradiation capsule. The Al foils that wrapped the sapphire containers were removed to avoid exposures to induced radioactivity from the Al foils. The containers were introduced into the SUS holders for transportation. In the original plan, we were going to measure gamma-rays of the irradiated samples to measure trace elements, but we gave up this measurement because of misfortune. Limited amounts of the irradiated samples were trans-ferred to Kyushu Univ., without detectable radioactivity from the samples. Each of the samples was picked up and placed into Al capsules for weighing and noble gas measurements (Fig. 2). The samples were installed into the vacuum system of the noble gas mass spectrometer at Kyushu Univ. Noble gas measurements are currently in progress.

Fig. 1. Meteorite samples and mineral standards in the sapphire containers wrapped with Al foils.

Fig. 2. Irradiated meteorite plagioclase (left column) and pyroxene (right column) samples in the Al foil capsules. The width of each photo is approximately 1 mm.

REFERENCES:

[1] E. Jarosewich *et al.*, Smithsonian Contributions to the Earth Sciences, **27** (1987) 1-49.

[2] S. Weiss, Mineralien Magasin Lapis. **16** (1991) 13-14.

CO5-8 ^{40}Ar-^{39}Ar Dating of Extraterrestrial Materials in KURNS

N. Iwata, S. Sekimoto[1], M. Inagaki[1], Y. N. Miura[2] and R. Okazaki[3]

Faculty of Science, Yamagata University
[1]Institute for Integrated Radiation and Nuclear Science, Kyoto University
[2]Earthquake Research Institute, University of Tokyo
[3]Department of Earth and Planetary Sciences, Kyushu University

INTRODUCTION: Radiometric dating is a valuable tool for unveiling the formation and evolution process of planetary material. The K-Ar and ^{40}Ar-^{39}Ar methods are invaluable to date the timing of heating events on planetesimals and asteroids (e.g. Swindle et al. (2014) [1]). The ^{40}Ar-^{39}Ar dating method with laser heating technique is suitable for tiny samples (e.g. Kelley, 1995 [2] and Hyodo, 2008 [3]). To date the extraterrestrial material by the ^{40}Ar-^{39}Ar method in KURNS, we have continued developing a ^{40}Ar-^{39}Ar dating system which includes laser-heating gas extraction and gas purification line.
Fig. 1 shows the latest schematic drawing of the system. A continuous Nd-YAG laser (~15 W) extracts gas from a neutron-irradiated sample. The extracted gas is purified using a Sorb-AC getter pump in the purification part. After the purification of extracted gas, argon isotope ratios in the gases are analyzed using an online connected quadrupole mass spectrometer. The whole of the extraction and purification parts will be evacuated by a rotary oil pump, two turbomolecular pumps and an ion pump to an ultra-high vacuum condition.

EXPERIMENTS & RESULTS: We have continued assembling the gas extraction and purification system in FY2022. Then, we could evacuate the extraction and purification parts. Pressure in the vacuum plumbing lines reaches 10^{-6} Pa at N1 on the top of the turbomolecular pump and 10^{-4} Pa at N2 under pumping (Fig. 1). The vacuum quality is several orders of magnitude higher than that of the ideal, insufficient to ^{40}Ar-^{39}Ar dating in KURNS. Bakeout is necessary to attain ultra-high vacuum conditions of the system. The vacuum condition (i.e., amounts of interfering isotopes) and the sensitivity of the quadrupole mass spectrometer (QMS) equipped with the system determine the amounts of samples required for analysis. Hence, the next step is to install the QMS to evaluate these factors.

REFERENCES:
[1] T. D. Swindle *et al.*, in Advances in ^{40}Ar/^{39}Ar Dating: from Archaeology *to Planetary Sciences*, edited by Jourdan, Mark, Verati (Geol. Soc., London, Spec. Pub. **378**, 2014) 333-347.
[2] S. P. Kelley, in Microprobe techniques in the earth sciences, edited by Potts, Bowles, Reed, Cave (Chapman & Hall, London, 1995) 327-358.
[3] H. Hyodo., Gondwana Res. **14** (2008) 609-616.

Explanation of Fig. 1. Latest schematic diagram of gas extraction and purification line in KURNS. RP, TMP, IP and Sorb-AC denote rotary pump, turbomolecular pump, ion pump and Sorb-AC getter pump, respectively. P1 and P2 are Pirani gauges. N1 and N2 are nude Bayard-Alpert ion gauges. CH denotes charcoal trap. QMS indicates quadrupole mass spectrometer. Equipment marked with dashed lines (QMS, CH, RP) is the forthcoming component.

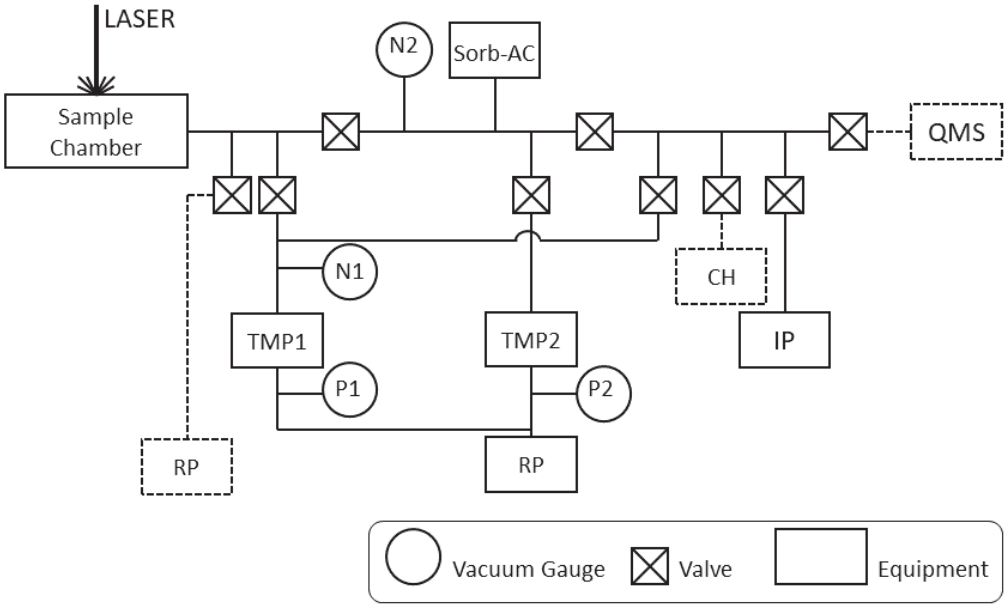

Fig. 1. Latest schematic diagram of gas extraction and purification line in KURNS.

CO5-9 Determination of Abundance of Rare Metal Elements in Seafloor Hydrothermal Ore Deposits by INAA Techniques-9: Behaviour of trace metal elements in gold-rich hydrotthermal ore deposits

J. Ishibashi, K. Kohama[1], K. Yonezu[1], T. Nozaki[2], R. Okumura[3], Y. Iinuma[3], H. Yoshinaga[3] and K. Takamiya[3]

Ocean-bottom Exploration Center, Kobe University
[1]Department of Earth Resources Engineering, Faculty of Engineering, Kyushu University
[2]Submarine Resources Research Center, Research Institute for Marine Resources Utilization, Japan Agency for Marine-Earth Science and Technology (JAMSTEC)
[3]Institute for Integrated Radiation and Nuclear Science, Kyoto University

INTRODUCTION: Instrumental neutron activation analysis (INAA) has several advantages for geochemical tools to provide useful information for mineral exploration. INAA enables highly sensitive multi-element analysis without geochemical pretreatment. We have conducted studies using mineralized samples collected from seafloor hydrothermal deposits, with a view to extend the range of application of this technique. Here, we report results of INAA analysis of some ores collected from a hydrothermal filed where occurrence of gold-rich ores had been reported [1].

SAMPLES: Ore samples collected from an active seafloor hydrothermal field on a submarine caldera volcano in Izu-Bonin Arc were provided for the study. Within the caldera, three active hydrothermal fields, Central Cone (CC) Site, South East (SE) Site and East (ES) Site, have been located. While CC site is located near the central cone, the other two sites are along the caldera wall.

EXPERIMENTS: INAA analysis was conducted by two runs. For short life nuclides, powdered samples of 10-20 mg were irradiated at Pn-3 (thermal neutron flux = 4.68×10^{12} n/cm^2/sec) for 30 seconds, and the gamma ray activity was measured for 3 minutes after adequate cooling time (3~15 minutes). For long life nuclides, powdered samples of 10-20 mg were irradiated at Pn-2 (thermal neutron flux = 5.50×10^{12} n/cm^2/sec) for 30 minutes, and the gamma ray activity was measured for 15 minutes after adequate cooling time (~30 hours).

RESULTS: As shown in Fig. 1, some interest correlations were recognized among concentrations of metal elements in the ores. Concentration of Au showed poor correlation with Zn regardless of the sampling sites (Fig. 1A). This correlation is in accordance with Au mineralization style as native Au or electrum, considering that Zn is the dominant element of the collected sulfide ores. Correlation between Ag and Sb concentrations (Fig. 1B) would be interpreted as a result of replacement in the tetrahedrite-tennantite system where Cu+As is replaced by Ag+Sb. These notable correlations suggest substantially high concentrations of Au and Ag in the hydrothermal fluid. For trace elements, In was detectable only for the SE and ES Sites showing correlation with Zn (Fig. 1C), whereas Co was detectable only for CC Site showing correlation with Fe (Fig. 1D). These correlations could be attributed to a result of replacement in the host sulfide minerals such as sphalerite and pyrite. Recognition of these trace elements in specific sites could be attributed to difference in chemical condition of the hydrothermal fluid among these three sites.

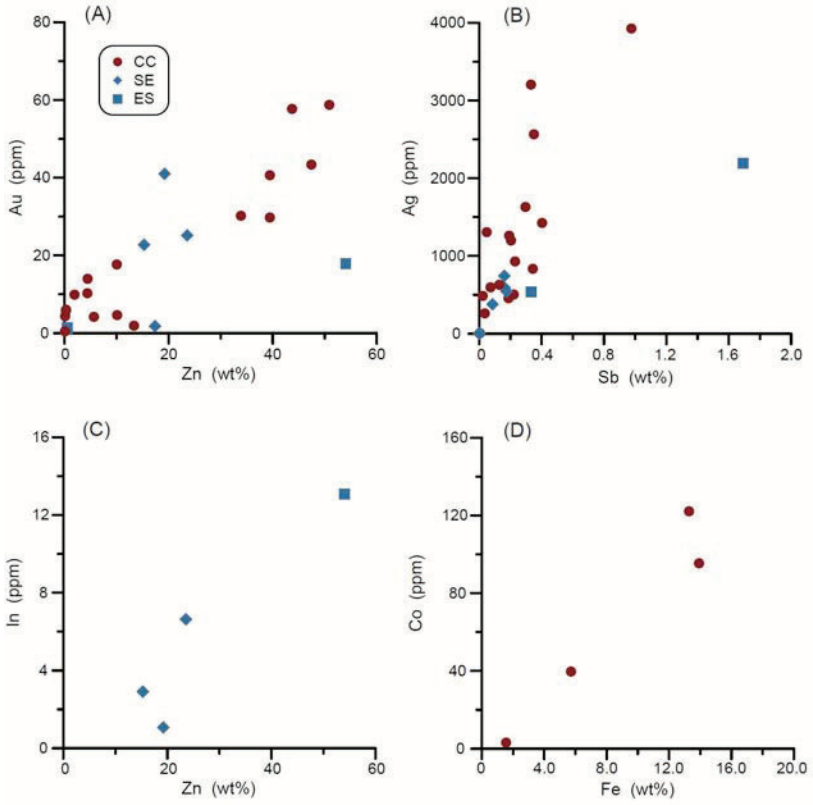

Fig. 1. Relationship between metal element concentrations of the ores. (A) Au vs Zn, (B) Ag vs Sb, (C) In vs Zn, (D) Co vs Fe

REFERENCES:

[1] K. Iizasa *et al.*, Mineralium Deposita, **54** (2019) 117-132.

CO5-10 Size distribution of metal elements in the atmospheric aerosols

N. Ito, A. Mizohata, Y. Iimura[1], H. Yoshinaga[1]

Radiation Research Center, Osaka Metropolitan University,[1] Institute for Integrated Radiation and Nuclear Science, Kyoto University

The atmospheric aerosols, the suspended particles existing anywhere in the atmosphere on the size range of 10nm-100 μm, effect our health by their depot ion(mainly fine particle) on the respiration tract and the lung, and also effect the climate by their absorption and reflect of the Sun light. To observe the size distribution and the chemical constituents of the atmospheric aerosols for the long period provide the data to analyze the air pollution effect to our health and the cause of global warming.

We have observed the atmospheric aerosols since 1995 at Sakai,Osaka and analyze the chemical components(ions,carbon elements and metals) in the atmospheric aerosols. In this report we show the size distribution data(central diameter) of the elements, which were analyzed by the neutron activation analysis using Kyoto University nuclear reactor.

We have collected the samples of the atmospheric aerosols by Andersen sampler, which collect the samples by 9 size rages(>11 μm ,11-7,7-4.7 μm ,4.7-3.3μm , 3.3-2.1,μm, 2.1-1.1 μm ,1.1-0.65 μm ,0.65-0.43μm ,<0.43μm) on the 1 week period at Osaka Metropolitan University(Osaka,Sakai). General size distribution of mass of the atmospheric aerosols, which have two peaks, fine(<2μm) and coarse(>2μm), is shown on Fig.1. Fine particles (atmospheric aerosols <2 μm m) are almost ions and carbon elements(organic and elementary carbon) and few of metals. Fine particles are produced by burning and chemical process from gaseous materials. Coarse particles(atmospheric aerosols > 2μm) are mainly soil particle and sea salt particles.

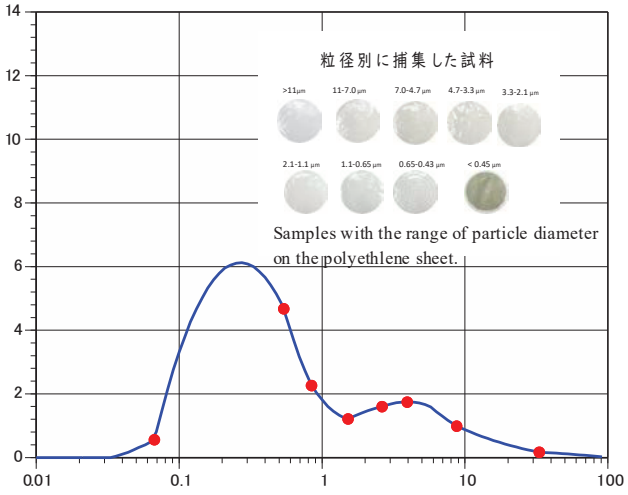

Fig.1. Example of mass size distribution of the atmosphe ric aerosols observed at Sakai, Osaka. The aerosols are cl lected by 9 size ranges.

We show the example of the size distribution of metal,V (Fig.2). The central diameter is the peak of fine particles. Result of the central diameter averaged by 70 samples from 1995 for the elements is shown via element melting point (Fig.3). The melting point of element relates to the creation of particles by the process of burning and emission from burning system.

From Fig3.,we can guess that the decrease trend of central diameter imples that high melting point element can makes fine particles that central diameter is smaller than 0.4μm. In the observed elements V and Mo which might be emitted from oil burning process, has smallest diameter and high melting point .

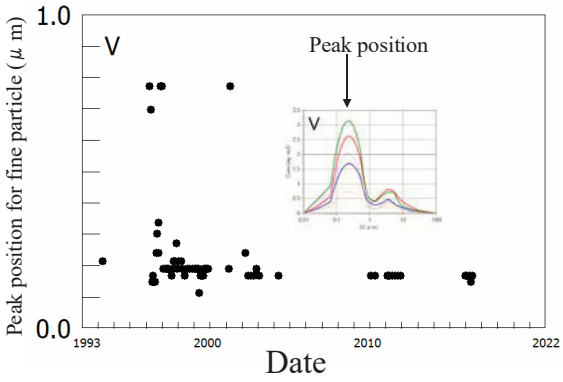

Fig.2. Central peraks and their yearly chage in va nadium(V) in the atmospheric aerosols observed at Sakai,Osaka.

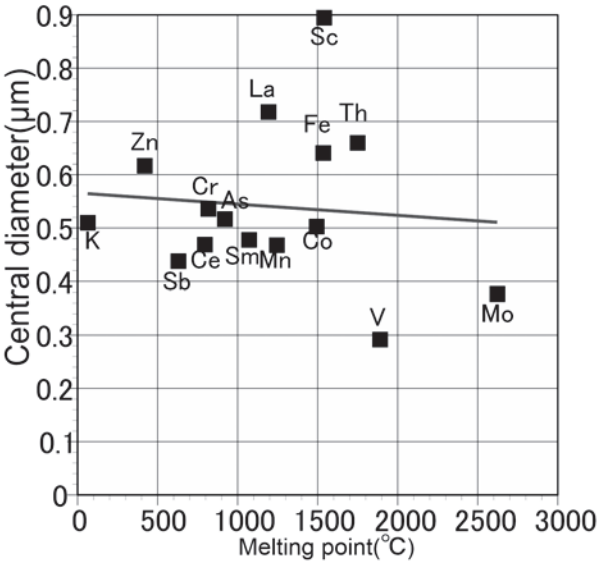

Fig. 3. Scatter graph on the central diameter and m elting point of the elements mainly observed in the fine particles.

CO5-11 Absorption of alkali metal ions by white radish sprouts (IV)

M. Yanaga, Y. Oshiro[1], T. Nakamura[1], H. Yoshinaga[2], R. Okumura[2] and Y. Iinuma[2]

Center for Radioscience Education and Research, Faculty of Science, Shizuoka University

[1]*Department of Chemistry, Faculty of Science, Shizuoka University*

[2]*Institute for Integrated Radiation and Nuclear Science, Kyoto University*

INTRODUCTION: More than 10 years after the Fukushima Daiichi Nuclear Power Plant accident, radioactive cesium still exists in the soil of the fields, and it is the cause of the harmful rumors. Separating radioactive cesium from the soil is necessary to prevent damage by rumors and to minimize the quantity of radioactive waste because simply removing the contaminated soil will result in a large amount of radioactive waste. Our previous reports have shown that the absorption of radioactive cesium ions from contaminated soil into rice plants increased by adding stable cesium ions to irrigation water, and that the possibility that the cesium ions added were replaced with radioactive cesium ions in soil [1, 2]. On the other hand, it was also found that addition of excess amount of stable cesium caused an obstacle to growth of rice plant [3].

We examined the removal of radiocesium from two types of soil, kuroboku soil (Andsols) and vermiculite, which were artificially contaminated with ^{137}Cs, through chemical treatment with various kinds of alkali ion solutions. The effect of decontamination with alkaline ions on the growth of plants was also investigated for white radish sprouts as model plants. In investigation of the behavior of trace elements in white radish sprouts, simulated decontamination with alkaline ions was performed on the soil containing no radioactive cesium and examined. White radish sprouts were also cultivated hydroponically in order to investigate the influence of alkali metal ions.

EXPERIMENTS: *^{137}Cs removal from soil* A sample (30 g) of commercially obtained vermiculite or kuroboku soil was placed in a metal mesh, immersed in 300 mL of aq. ^{137}Cs (10 Bq/mL) solution for one day, then removed from the solution and dried. After that, 35 mL of 0.014 mol/L KCl, RbCl or CsCl solution were added to a cen-trifuge tube containing 18 g of the contaminated soil and the mixture was stirred for 72 hours. Each soil was re-moved by filtration, then, washed with pure water. The same treatments were also applied to soil that was not contaminated with radioactive cesium.

Materials and Method The dried each soil mentioned above was placed in a plastic pot, wetted with pure water and 1.0 g of radish sprouts seeds were sown on it. After germination, Hyponex□ diluted 2000 times was added as liquid fertilizer. After that, they were cultivated for 4 - 5 days while giving only pure water as appropriate. White radish sprouts cultivated in soil without radioactive cesium were subjected to INAA. In hydroponics, seeds were sown on absorbent cotton and 30 mL of pure water was added. After germination, 10 mL of different concentrations (1.0×10^{-6} – 2.5×10^{-3} mol/L) of each alkali metal ions were added twice.

INAA The samples in polyethylene capsules were irradiated in Pn-3 for 90 seconds and in Pn-2 for 4 hours, for short and long irradiation, respectively. As comparative standards, the certified NIST Standard Reference Ma-te-rial 1577b Bovine Liver as well as elemental standard for Cs was used. The γ-ray spectroscopic measurements with an HPGe detector were performed repeatedly for the short-irradiated samples: the first measurements for 120 – 900 seconds after decay time of 5 - 15 minutes and the second one for 250 - 1200 seconds after 60 - 150 minutes. The long-irradiated samples were measured for 1 - 24 hours after an adequate cooling time (15 - 60 days).

RESULTS: Experimental results for removing radioactive cesium from soil showed that 10% or more of radioactive cesium was removed using any alkali metal ion. More than 20% of radioactive cesium was removed from vermiculite when rubidium ions or cesium ions were used. However, this high decontamination rate may be due to the fact that cesium ions are not strongly bound to vermiculite under the conditions in this experiment. When each soil that had been decontaminated once was washed with pure water, radioactive cesium was further removed, confirming that washing with water after decontamination is effective. The transfer coefficients of radioactive cesium to radish sprouts grown in soil after decontamination ranged from 0.03 to 0.16, and high transfer coefficients were shown when rubidium or cesium ions were used as decontamination agents.

The concentration of potassium ions in the hydroponically cultivated radish sprouts was decreased as the concentration of added rubidium ions or cesium ions increased, indicating a competitive relationship. However, the decrease in potassium ion concentration was not significant, but rather remained almost constant. On the other hand, the chloride ion concentration showed a different trend. Chloride ion concentration was almost constant when the added alkali metal ion (and chloride ion) concentration was in the range of 1.0×10^{-6} – 2.5×10^{-4} mol/L. However, above this range, significantly higher concentrations were shown. This indicates that changes in trace element concentration may indicate abnormalities even when no growth disorder is apparently observed. It is considered that exposure to the high-concentration solution caused abnormalities in the uptake mechanism of young roots.

REFERENCES:

[1] M. Yanaga *et al.*, NMCC ANNUAL REPORT, **22** (2015)185-190.
[2] M. Yanaga *et al.*, NMCC ANNUAL REPORT, **23** (2016)172-179.
[3] M. Yanaga *et al.*, KURNS Progress Report 2018 (2019) CO5-10.

CO5-12 Basic Study on Trace Elemental Analysis of Airborne Particulate Matters in an Environment by INAA & PIXE

N. Hagura[1,2,3], T. Matsui[3], T. Uchiyama[2], H. Matsuura[1,2,3]

[1] Nuclear Safety Engineering, Science and Engineering, Tokyo City University
[2] Atomic Energy Research Laboratory, Science and Engineering, Tokyo City University
[3] Cooperative Major in Nuclear Energy, Integrative Science and Engineering, Tokyo City University

INTRODUCTION: To discuss the elemental distribution of airborne particulate maters (APM) in an environment with large variability, it is necessary to accumulate a large amount of measurement data. Therefore, a sufficiently long time and a large number of samples are required. In order to efficiently perform a large number of measurements and analysis, we believe that it is important to use ion beam analysis methods in parallel with an analytical method using a nuclear reactor.
The Atomic Energy Research Laboratory of Tokyo City University (TCU-AERL) operated the Musashi reactor until 1989 and has been conducting research using neutrons, including instrumental neutron activation analysis (INAA). Although now it is in the decommissioning phase, the facility is still in operation as a facility for conducting experiments using RI. Since 2002, sampling of airborne particulate matter have been performed on our facility. In 2018, a 1.7 MV Pelletron tandem accelerator (TCU-Tandem) was installed and began performing trace element analysis using Particle Induced X-ray Emission (PIXE) [1].
In near future, unfortunately it may become increasingly difficult to conduct experiments using research reactors. Therefore, we believe that the use of accelerator ion beams is an effective means of advancing analytical methods. In addition, ion beam analysis is expected to provide more valuable measurement data, including information on chemical bonding states.
In this study, trace element analysis by instrumental neutron activation analysis and measurement by ion beam analysis using a tandem accelerator were conducted on the APM samples. And also we have considered a system concept that enables measurement with energy resolution at a level that can determine chemical form, namely, wavelength dispersive spectroscopy PIXE (WDS-PIXE) analysis method.

EXPERIMENTS: The sampling method for airborne particulate matters is explained. We use a high volume air sampler (Shibata Scientific Technology LTD., HV-1000F, filter: ADVANTEC, QR-100 (collection efficiency: 99.99% for 0.3 μm particles)) with an inhalation flow rate of 700 L min^{-1}. The radioactivity of the filter that has collected dust is measured by a high-purity germanium (HP-Ge) semiconductor detector, and a part of the filter was stored for INAA.
The conditions of the INAA method are described. Irradiation was performed at the research reactor KUR at the Institute for Integrated Radiation and Nuclear Science, Kyoto University, between the December and February with four machine times in FY2022. The irradiation conditions are shown in Table 1. The measurement of radioactivity of short half-life nuclides was carried out using the HP-Ge semiconductor detector of the hot laboratory of KUR. And long and medium half-life nuclides, after cooling for one or two weeks, transported to the TCU-AERL, and was measured by a HP-Ge semiconductor detector. JLk-1 and others were used as a comparative standard substance.

RESULTS: This year, several samples of stocked airborne dust from 2011, 2016, 2017, and 2018 were measured. In addition, PIXE analysis is being conducted at TCU-Tandem. We plan to summarize the data together with the results of past measurements. Figure 1 shows the concept of a wavelength-dispersive spectroscopy PIXE (WDS-PIXE) analysis system [2]. This concept is characterized by the application of image processing techniques to the acquisition of X-ray bright spots to improve positional resolution. The aim is to achieve high energy resolution while maintaining a compact size. We have constructed an analytical chamber and confirmed that it is possible to cover the target elemental range in the measurement of atmospheric airborne dust samples by appropriately selecting spectroscopic crystals.

Table 1. Irradiation conditions.

Irradiation			Operating power	Thermal neutron flux
date	time	position		
2022/12/6	60 min	Pn-2	1 MW	5.5 x 10^{12} n/cm^2/sec
2023/1/24	60 min	Pn-2		5.5 x 10^{12} n/cm^2/sec
2023/2/8	30 sec	Pn-3		4.7 x 10^{12} n/cm^2/sec
2023/2/14	60 min	Pn-2		5.5 x 10^{12} n/cm^2/sec

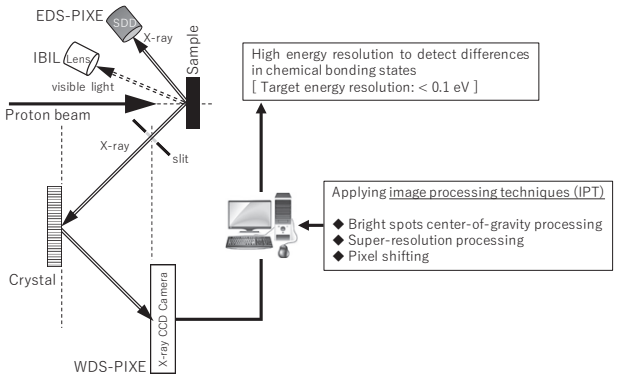

Fig. 1. Conceptual diagram of wavelength-dispersive spectroscopy PIXE analysis system [2] .

REFERENCES:

[1] N. Hagura *et al.,* Trans. At. Energy Soc. Japan, **17 (3-4)** (2018)111-117.
[2] K. Ushijima *et al.,* 2022 IEEE NSS MIC RTSD, (2021)NSS-20-154.

CO5-13 Ar-Ar Dating for Differentiated Meteorites

Y. N. Miura, R. Okazaki[1], S. Sekimoto[2], M. Inagaki[2] and N. Iwata[3]

Earthquake Research Institute, University of Tokyo
[1]Earth and Planetary Sciences, Kyushu University
[2]Institute for Integrated Radiation and Nuclear Science, Kyoto University
[3]Faculty of Science, Yamagata University

INTRODUCTION: Extra-terrestrial materials, such as meteorites and samples collected by asteroid/planetary explorations, provide a variety of information for understanding the origin and evolution of the solar system. In particular, age determination gives us direct knowledge about thermal histories as well as timing of the events occurred in solar nebular and on the parent bodies (e.g., [1, 2]). The K-Ar/Ar-Ar ages (a chronometer based on the ^{40}K-^{40}Ar pair) likely correspond to thermal metamorphism, aqueous alteration or impact heating on the parent bodies (e.g., [3]). The Ar-Ar dating method, a variant of K–Ar dating, uses ^{39}Ar as a proxy for ^{40}K; ^{39}K is converted partly to ^{39}Ar by irradiation of fast neutrons. Therefore, Ar-Ar ages can be determined by ^{40}Ar/^{39}Ar ratios for a common spot between K and Ar. In addition, reliability of the ages are examined by age spectra obtained from the step-heating method, that is a sample is heated stepwisely and released Ar of each step is measured. In order to perform Ar-Ar dating for extra-terrestrial samples, we attempt to establish the analytical protocol and apparatus at KURNS. A system consisting of gas extraction, gas purification and Ar isotope measurements is being constructed.

EXPERIMENTS and RESULTS: The gas extraction/purification line is composed of a CW Nd:YAG laser, a Sorb-ac getter, two vacuum gauges, two turbo molecular pumps (each TMP equips with a rotary pump and a pirani gauge), an ion pump, valves and connection parts (Fig. 1). For Ar isotope measurements we are preparing a quadrupole mass spectrometer (QMS), which is now attached to a vacuum line at University of Tokyo and will be connected to the line at KURNS in FY2023. Usefulness of QMS has been reported for K-Ar/Ar-Ar dating (e.g., [4-6]). The gas extraction/purification line was evacuated by the two turbo molecular pumps and its vacuum pressure reached to 10^{-6} Pa near the vacuum pump and to 10^{-4} Pa at the gas purification line (near the Sorb-ac getter). In order to measure Ar isotopes for Ar-Ar dating, vacuum condition has to be improved by bakeout and degassing the Sorb-ac getter. The Nd:YAG laser (maximum output power ~15W) was set up by attaching objective lens, eyepiece lens and an optical light (Fig. 2, a picture of the laser before attaching eyepiece lens and the optical light). Laser irradiation was performed to a test piece. During the test irradiation we controlled output power still low so that it was not enough to melt rock samples. We will adjust optical alignment and apply laser-irradiation with higher power to rock samples.

Fig. 1 A picture of the gas extraction/purification line. The line was evacuated by two turbo molecular pumps. The vacuum pressure was monitored by two ion gauges. A QMS and a sample chamber will be connected to ICF34 ports of the line.

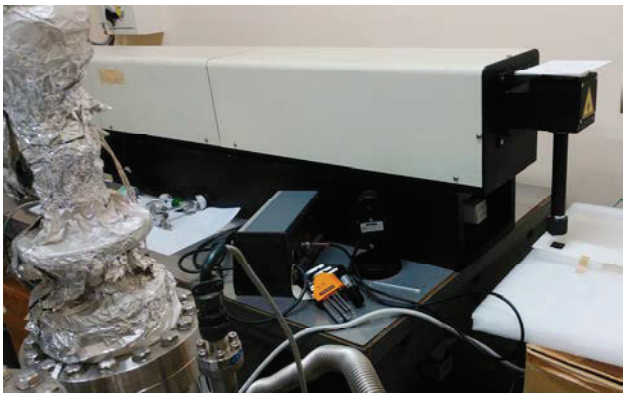

Fig 2. A picture of the CW Nd:YAG laser, which is under setup processes and will be used for extraction of Ar from rock samples.

REFERENCES:

[1] D. S. Lauretta and H. Y. McSween, Meteorites and the Early Solar System II (Space Science Series, Univ. of Arizona Press) (2006).
[2] A. Longobardo, Sample Return Missions: The Last Frontier of Solar System Exploration (Elsevier) (2021).
[3] D. Bogard, Chemie der Erde, **71** (2011) 207-226.
[4] B. Schneider *et al.,* Quaternary Geochronology, **4** (2009) 508-516.
[5] Y. Cho *et al.* Planet. Space Sci., **128** (2016) 14-29.
[6] Y. Cho and B. A. Cohen, Rap. Comm. Mass Spectrometry, **32** (2018) 1755-1765.

CO5-14 Halogen and noble gas characteristics of subcontinental lithospheric mantle beneath southwestern North America and northwestern Africa

H. Sumino, Y. Hibiya, M. Fukagawa[1], J. Ren[1], T. Oishi[1], A. Takenouchi[2], Y. IInuma[3], R. Okumura[3], H. Yoshinaga[3] and S. Sekimoto[3]

Research Center for Advanced Science and Technology, University of Tokyo
[1]Graduate School of Arts and Sciences, University of Tokyo
[2]Kyoto University Museum, Kyoto University
[3]Institute for Integrated Radiation and Nuclear Science, Kyoto University

INTRODUCTION: The subcontinental lithospheric mantle (SCLM) is generally metasomatized by intra-plate or arc magmatism, making them distinct geochemical reservoirs from mid-ocean ridge basalts (MORBs) and ocean island basalt (OIB) sources. Higher $^{3}He/^{22}Ne$ is observed in mantle-derived xenoliths from the SCLM in Patagonia, South America [1], compared to MORBs and OIBs, which reflect the composition of the convecting mantle and plume source, respectively. Based on this $^{3}He/^{22}Ne$ difference, SCLM is expected to be a distinct geochemical reservoir that has evolved differently from the convecting mantle and plume sources in terms of noble gases [2]. The average $^{3}He/^{4}He$ of SCLM-derived peridotite samples is about 6 Ra [3], where 1 Ra = 1.4×10^{-6} represents atmospheric $^{3}He/^{4}He$, suggesting that the contribution of radiogenic ^{4}He derived from the decay of U and Th to SCLM is more significant than that to the convecting mantle with $^{3}He/^{4}He$ of ca 8 Ra. In addition, Ne isotopic compositions of the SCLM samples from Patagonia in South America have been confirmed to have a more significant contribution of nucleogenic ^{21}Ne from $^{24}Mg[n,\alpha]^{21}Ne$ and $^{18}O[\alpha,n]^{21}Ne$ reactions compared to MORBs. If the SCLM is a globally homogeneous reservoir, these features are expected to be observed in SCLMs in other regions. Therefore we analyzed noble gases and halogens in SCLM-derived samples from the Lunar Crater volcanic field, Toroweap flow, the Mendocino Mountains, and Mount Emma in southwestern North America, and Beni Bousera peridotite body in northwestern Africa.

EXPERIMENTS: The samples of 5-50 mg each and standards for neutron fluence were wrapped with aluminum foil and put in aluminum capsules of ϕ10 mm x 30 mm. The capsules were irradiated with neutrons in KUR. After the irradiation, the samples were sent to the University of Tokyo. The samples were loaded into an ultrahigh-vacuum, noble gas extraction, purification, and separation line. Argon was extracted from the samples by heating up to 1800°C, purified with hot titanium-zirconium getters, separated into each noble gas with temperature-controlled cold traps, and then determined their isotope compositions with a noble gas mass spectrometer [4,5]. The fast neutron flux was estimated as $(1.0–1.2) \times 10^{18}$ neutrons cm^{-2}, from the production of ^{39}Ar from ^{39}K in the Hb3gr hornblende standard in which K contents have been determined by [8].

RESULTS: The samples from southwestern North America have $^{3}He/^{4}He$ that fall within the range of the convecting mantle. On the other hand, the $^{3}He/^{4}He$ ratios of the Beni Bousera peridotite samples are low, ranging from 0.3 Ra to 0.7 Ra. The Ne isotope ratios of the southwestern North America samples are also accounted for by mixing between air and convecting mantle endmembers. In contrast, those of the Beni Bousera peridotite samples suggest the addition of nucleogenic Ne to the atmospheric compositions. These results indicate that the SCLM is not a homogeneous geochemical reservoir of noble gases.
The MORB-like He and Ne feature of the samples from southwestern North America differs from those of other SCLMs. This result suggests that the SCLMs beneath these regions were incorporated into the mantle convection by delamination, resulting in compositional overwriting with the convecting mantle component. The contribution of nucleogenic ^{21}Ne correlates with that of radiogenic ^{4}He and is substantial in the Beni Bousera peridotite body samples. The sample was reported to have experienced deformation and dynamic recrystallization, which may have resulted in the loss of mantle-derived noble gases.
In contrast to the noble gas features, the Br/Cl and I/Cl ratios of the samples from southwestern North America and northwest Africa share similar characteristics in which Br/Cl and I/Cl range 1.2-7.8 $\times 10^{-3}$ mol/mol and 61-860 $\times 10^{-6}$ mol/mol, respectively, while I/Br showed fewer variations (0.031-0.110 mol/mol). Both samples are from the back-arc regions of the subduction zones, and a similar feature was observed for mantle-derived xenoliths in Takashima, northwestern Kyushu, Japan, which is also in the back-arc region. Therefore, it is possible that this feature is common in the back-arc regions of subduction zones and may result from Cl depletion in the mantle wedge having higher I/Cl due to the addition of iodine-rich subducted halogen component.

REFERENCES:
[1] T. Jalowitzki *et al.*, Earth Planet. Sci. Lett., **450** (2016) 263-273.
[2] N. Dygert *et al.*, Earth Planet. Sci. Lett., **498** (2018) 309-321.
[3] C. Gautheron, and M. Moreira, Earth Planet. Sci. Lett., **199** (2002) 39-47.
[4] N. Ebisawa *et al.*, J. Mass Spectrom. Soc. Jpn. **52** (2004) 219-229.
[5] M. Kobayashi *et al.*, Chem. Geol. **582** (2021) 120420.
[6] J. C. Roddick, Geochim. Cosmochim. Acta **47** (1983) 887-898.

CO5-15 Determination of Cl, Br and I contents in U. S. Geological Survey reference materials by RNAA

S. Shirai, S. Sekimoto[1], M. Ebihara[2]

Department of Chemistry, Faculty of Science, Kanagawa University
[1]Institute for Integrated Radiation and Nuclear Science, Kyoto University
[3]Department of Chemistry, Tokyo Metropolitan University

INTRODUCTION: Compared with other trace elements, cosmochemical and geochemical behaviors of halogen elements are still not well understood. The major reason is that there are a limited number of techniques available to precisely analyze the halogen contents in solid samples. As a result, large variations exist between the reported values in geological reference samples. Recently, ICP-MS has been commonly used for the determination of halogen contents. In this method, halogens are extracted from rock samples by pyrohydrolysis. As mentioned by Sekimoto and Ebihara [1], the quantitive collection of halogens cannot always be achieved by phrohydrolysis. In this study, halogen contents in rock samples are determined by radiochemical neutron activation analysis, and the obtained analytical results were evaluated.

EXPERIMENTS: Standard solutions of Cl, Br, and I were prepared by dissolving know amounts of chemical reagents (KCl, KBr, and KI) into high-purity water. For I, KOH was added to stabilize I^- in the solution. Chemical reference samples of three halogens were prepared by pipetting know amounts of these standard solutions onto filter papers.
BHVO-2 prepared U.S. Geological Survey was used in this study. This reference material was in powder and was not subjected to any additional treatment such drying. BHVO-2 weighing about 110 to 320 mg was weighed in a clean plastic vial. This geological reference materials together with a set of chemical reference samples of three halogens were irradiated with neutrons for 10 min. After cooling for 10 min, geological reference material was transferred into a Ni crucible, in which known amounts of the three halogen carriers in solution were taken and dried with a proper amount of concentrated NaOH solution. NaOH in pellets was added and heated gently for 3 min, then strongly for 5 min over a Mecker burner. After cooling for a few min, H_2O was added to the fusion cake. The precipitate was separated by centrifugation and Na_2SO_3 as a reductant was added to the obtained supernatant. 6M HNO_3 and $Pd(NO_3)_2$ in solution was added. The PdI_2 precipitate was collected onto filter paper. $AgNO_3$ in solution was added to the filtrate in order to precipitate Cl^- and Br^- as AgCl and AgBr. These precipitates were collected onto filter paper. These precipitates were dried under a heat lamp and measured for gamma rays. Chemical yields of the three halogens were determined by reactivation method. The precipitates were again irradiated with neutrons for a few seconds together with reference samples. After cooling, these samples were measured for gamma rays. The analytical procedure used in this study was essentially the same as those of Sekimoto and Ebihara [1].

RESULTS: Analytical results for the three halogens for BHVO-2 are indicated in Table 1, where literature values [2-5] are also shown for comparison. BHVO-2 was analyzed five times, and the mean values with one standard deviation repeatabilities are calculated and indicated. The three halogen contents were determined by using noble gas mass spectrometry (NG-MS) [2]. In this method, the samples were irradiated, and halogen-derived noble gas isotopes produced were analyzed. Three halogens were extracted from samples by pyrohydrolysis technique, and Cl, and Br and I were determined by ion chromatography and ICP-MS, respectively [3,4]. The analytical procedure used in [5] was the same as used in this study. As shown in Table 1, ion chromatography value for Cl [3] is higher than both literature values, and our data are consistent with literature values [2,4,5]. There are good agreements of Br values among our data and literature values. In contrast, there is a large deviation of I values. Our data are in agreement with NG-MS value [2], and inconsistent with other literature values [3-4]. There are no reasonable explanations for this discrepancy. As a careful preparation of chemical references of I was performed in this study, it is suggested that our values are more reliable.

REFERENCES:

[1] S. Sekimoto and M. Ebihara, Anal. Chem., **85** (2013) 6336-6341.
[2] M. A. Kendrick *et al.,* Geostand. Geoanal. Res., **42** (2018) 499-511.
[3] A. Michel and B. Villemant, Geostand. Geoanal. Res., **27** (2003) 163-171.
[4] H. Balcone-Boissard *et al.,* Geostand. Geoanal. Res., **33** (2009) 477-485.
[5] S. Sekimoto and M. Ebihara, Geostand. Geoanal. Res., **41** (2017) 213-219.

Table 1. Analytical results of three halogens (Cl, Br and I) in BHVO-2.

	Cl (ppm)	Br (ppm)	I (ppm)
This work (n = 5)	90.6±4.5	0.240±0.012	0.0592±0.0078
Kendrick et al. [2]	102±1	0.259±0.005	0.070±0.040
Michel and Villeman [3]	150±21	0.269, 0.277	0.016±0.002
Balcone-Boissard et al. [4]	81±11	0.29±0.10	0.020±0.012
Sekimoto and Ebihara [5]	104±1	0.240±0.013	0.307±0.050

CO5-16 Phase identification and amorphous structure analysis of chondrule-simulated samples

Y. Seto, T. Araga[1], Y. Tarutani[1], Y. Umeda[2], T. Okuchi[2]

Department of Geoscicences, Graduate School of Science, Osaka Metropolitan University
[1]Department of Mechanical Engineering and Science, Graduate School of Engineering, Kyoto University
[2]Institute for Integrated Radiation and Nuclear Science, Kyoto University

INTRODUCTION:

Chondrites are the most common type of meteorite that formed during the earliest period of the solar system. They contain spherical objects, called chondrules, with diameters ranging from 0.1 to 10mm. Chondrules are thought to have formed when aggregates of dust that coalesced and grew within the protoplanetary disk melted due to instantaneous heating, and then rapidly cooled.

It is believed that chondrules were primarily composed of glassy or low-crystallinity silicates, but their internal texture changed due to various subsequent processes (re-melting, shock-induced metamorphism, thermal metamorphism) after their formation. Unraveling the process of these changes is an important clue to deciphering the material evolution of the early solar system.

The reaction of silicate glasses to heat and shock is, however, generally slow and difficult to reproduce in the laboratory. In this study, we used GeO_2 glass as an analog of the chondrule to examine how crystallization proceeds in response to shock compression.

EXPERIMENTS:

GeO_2 glass samples were prepared by placing pelletized GeO_2 powder in a platinum container, heating and melting it at 1300-1450°C for 8-24 hours using a vertical tube furnace (at Osaka Metropolitan University) and quenching it under air.

The glass samples were carefully pulverized in a mortar, sealed in a stainless-steel container, and then subjected to shock compression (maximum pressure of 17 GPa) by striking a projectile using a single-stage powder gun (at National Institute for Materials Science).

Diffraction profiles of the samples before and after the impact compression were obtained using a fully automated multi-purpose X-ray diffractometer (Rigaku SmartLab) in the range of 5° to 120° using Cu Kα rotation anode X-ray tube. The profiles were analyzed using the software PDIndexer [1].

RESULTS and DISCUSSION:

In the diffraction profile of the glass sample before shock compression (blue line in Figure 1), there are no distinct diffraction peaks, and a halo pattern characteristic of the short-range order structure in amorphous materials can be observed.

On the other hand, in the profile after impact compression (orange line in Figure 1), slightly broad but distinct diffraction peaks were observed. Comparing the diffraction peaks with known crystal phases of GeO_2 revealed that most of them could be indexed by the quartz structure, but there were also peaks derived from the rutile structure. In the quartz structure, Ge is four-coordinated with surrounding oxygen, whereas in the rutile structure, it is six-coordinated. The latter structure exhibits a higher density compared to the former.

The present shock compression experiments and analyses of X-ray diffraction profiles show that GeO_2 glass can easily crystallize and change to a dense structure. Since the timescale of shock events in the solar system is much longer than that of laboratory shock compression experiments, it is quite possible that such crystallization and densification can occur even in silicate glasses, which have slower crystallization kinetics. In fact, a number of dense silicate minerals have been found in impact melts in meteorites [2,3]. We plan to further investigate the crystallization process of amorphous materials during shock compression by changing the shock pressure and the chemical composition of the starting materials.

REFERENCES:

[1] Seto *et al.*, Rev. High Press. Sci. Technol., **20** (2010) 269-276.
[2] Tomioka and Okuchi, Sci. Rep., **7** (2017) 17351.
[3] Tschauner *et al.*, Science, **346(6213)** (2014) 1100-2.

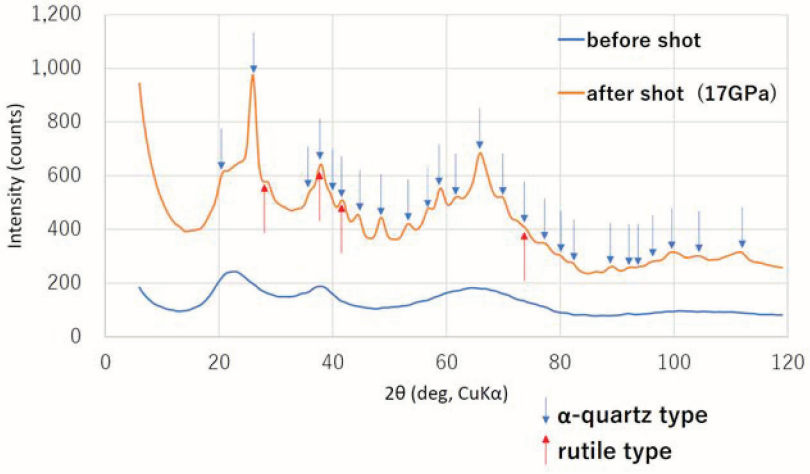

Fig. 1. Diffraction profiles of the GeO_2 samples before (blue) and after (orange) the impact compression. Before the shock, a halo pattern characteristic of glass materials was observed, but after the shock, a slightly broad diffraction peak was observed.

CO5-17 Distribution of radiocesium in forestry area in Fukushima -focusing on inner bark-

T. Ohta, S. Fukutani[1], T. Kubota[2], Y. Mahara[3]

Department of Nuclear Technology, Nagaoka University of Technology
[1] Institute for Integrated Radiation and Nuclear Science, Kyoto University
[2] Agency for Health, Safety and Environment, Kyoto University
[3] Kyoto University

INTRODUCTION: Vast forest was markedly contaminated by radioactive plums containing radiocesium in the wide range of the eastern part of Japan in 2011 [1–7]. As forests have an important role in preventing landslides and maintaining the ecological and hydrological system, the destructive forest should be avoided and an appropriately managed tree-felling should be conducted. It is necessary to know the environmental dynamics of radiocesium in forest to keep the forestry vividly.

In our previous field study [1], most of the radiocesium in the tree rings was directly absorbed by the atmospheric direct uptake via the bark and leaves rather than by roots. The chemical form of radiocesium on the leaves and bark would have been a mixture of water-soluble and insoluble forms. Another our previous study [2] demonstrated that the effluence rate of radiocesium (^{137}Cs) obtained from dissolved assay experiments on the trunks of *Cryptomeria japonica (Japanese cedar)*, indicating that the radiocesium in the trees was mainly water-soluble. We also directly measured root distribution of *Cryptomeria japonica*[3], indicating that mature it is not effective to absorb radiocesium by the root uptake due to the distribution of the fine root[3, 5].

After the accident, radioactive cesium was efficiently absorbed from the bark into xylem, but it is believed that the radioactive cesium in the bark does not migrate after that. Without a route from the inner bark to the xylem, radioactive cesium will remain on the surface of the xylem in the future. We measured the concentration of radioactive cesium the inner bark outside the xylem.

EXPERIMENTS: Barks were collected at the Koriyama, Fukushima. *Quercus serrata* was harvested prior to leaf fall at the end of September 2012 and *Cryptomeria japonica* was harvested at the end of October 2012. After cutting the trees, we carefully and completely stripped off all bark from the tree trunk. The collected the samples in the field were transported to the laboratory and stored it in the dark for 11 years. After separating the outer and inner bark, the ^{137}Cs in the inner bark was determined by gamma-ray spectrometry (HPGe). The concentration of ^{137}Cs was corrected on March 12, 2011.

RESULTS: Fig. 1.(a) and (b) show concentration of ^{137}Cs in the inner bark of the *Cryptomeria japonica* and *Quer-cus serrata*, respectively. The concentration of the ^{137}Cs in the inner bark of the *Cryptomeria japonica* was higher than that in the *Quercus serrata*. These may also depend on the ease of aerosol penetration and the shape of the bark.

The concentration of the xylem at the same site was less than 50Bq/kg collected in 2014 in the same site. The concentration of radiocesium did not increase from 2012 to 2014. The concentrations in the inner bark of the *Cryptomeria japonica* were three orders of magnitude higher than those in the xylem. We concluded that the radioceisum was not absorbed from not only the root but also inner bark effectively. However, our target trees are mature trees, and there is no guarantee whether the same tendency is observed in young trees.

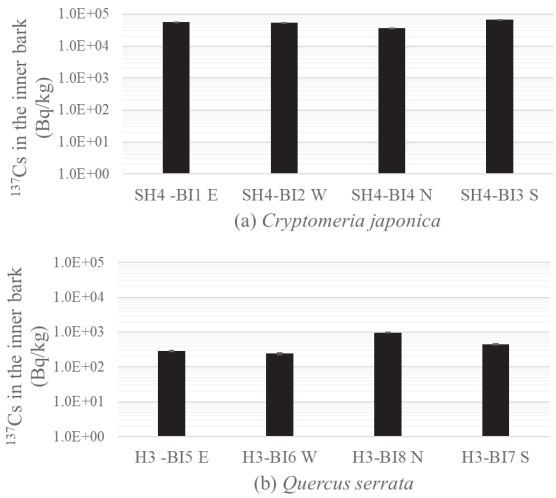

Fig. 1. Concentration of ^{137}Cs in the inner bark

REFERENCES:

[1] Y. Mahara *et al.,* Sci. Rep., **4** (2014) 7121.
[2] T. Ohta *et al.,* J. Radioanal. Nucl. Chem., **310** (2016) 109-115.
[3] Y. Mahara *et al.,* Sci. Rep., **11** (2021) 8404
[4] T. Ohta *et al.,* Radiological Issues for Fukushima's Revitalized Future, edited by T. Takahasi (Springer, 2016) 13-24.
[5] T. Ohta *et al.,* KURNS Progress Report 2021, p151
[6] T. Ohta *et al.,* Ana. Sci., **29** (2014) 941-947
[7] T. Ohta *et al.,* J. Environ. Radioact., **111** (2012) 38-41